

Backstepping control in speed loop combined with load torque observer-ESO for IPMSM in electric vehicle

An Thi Hoai Thu Anh¹, Tran Hung Cuong², Nguyen Van Hoa¹

¹Faculty of Electrical and Electronics Engineering, University of Transport and Communications, Hanoi, Vietnam

²Faculty of Electrical and Electronic Engineering, Thuyloi University, Hanoi, Vietnam

Article Info

Article history:

Received Oct 25, 2024

Revised Oct 3, 2025

Accepted Oct 17, 2025

Keywords:

Backstepping

Extended state observer

Interior permanent magnet synchronous motor

Load torque of electric vehicle

Sliding mode control

ABSTRACT

Electric vehicles are gaining popularity due to their environmental friendliness and the need to conserve dwindling fossil fuel resources. In this field, interior permanent magnet (IPM) motors are considered the top choice for propulsion systems due to their high efficiency, high torque-to-current ratio, durability, and low noise. To optimize the speed control performance of IPM motors in the presence of disturbances, a nonlinear speed control algorithm for IPM systems using the backstepping method is developed in this paper. Additionally, a load torque observer using the extended state observer (ESO) method is implemented to enable the system to respond quickly and accurately to load changes while minimizing the effects of disturbances, thereby enhancing the operation and reliability of electric vehicles. The simulation results, conducted in MATLAB/Simulink, demonstrate that the combination of backstepping control and ESO offers good stability for the motor system, while mitigating the impact of disturbances and load variations. This is an important step in optimizing the control system of electric vehicles, contributing to the improvement of performance and reliability in electric vehicle applications.

This is an open access article under the [CC BY-SA](https://creativecommons.org/licenses/by-sa/4.0/) license.



Corresponding Author:

Tran Hung Cuong

Faculty of Electrical and Electronic Engineering, Thuyloi University

Hanoi, Vietnam

Email: cuongth@tlu.edu.vn

1. INTRODUCTION

In the 21st century, the development and application of electric vehicle (EV) technology have become a prominent trend in the automotive industry. Electric vehicles help reduce environmental pollution, conserve fossil fuel resources, and provide high operational efficiency [1]. With high efficiency, torque generation capabilities, and a wide range of speed adjustments, interior permanent magnet (IPM) synchronous motors are optimal for electric vehicle propulsion systems. IPM motors are often controlled by proportional–integral (PI) or proportional–integral–derivative (PID) controllers, but they suffer from drawbacks such as susceptibility to parameter disturbances, inadequate adaptability to load changes, and weak noise immunity [2]. Therefore, many nonlinear control methods have been applied to improve control performance in systems with disturbances and parameter variations, such as adaptive fuzzy sliding control [3], [4], intelligent control [5], backstepping control [6], and Direct predictive speed control [7]. Among these methods, backstepping demonstrates a relatively simple controller, allowing for gradual computation through several steps, with feedback control making the closed-loop system stable according to Lyapunov theory. At each step, a virtual control variable is selected, and intermediate control laws are designed to stabilize the subsystem of the original system [8].

Controlling IPM motors also faces challenges due to nonlinearity in the model and load torque disturbances. Achieving high controller performance requires accurate measurement and determination of unknown parameters [9]. Load torque is essential for monitoring operational states to improve motor efficiency. Sensors can directly measure it, but direct measurement has many shortcomings, and installing sensors is also difficult (challenges in construction, high installation costs, and reduced mechanical system durability); in many cases, it is even impossible to install sensors [10], [11]. Additionally, changes in terrain during movement and the impact of external forces and disturbances pose challenges in load measurement. With vehicle loads, the vehicle is influenced by rolling resistance, friction, inertia, and aerodynamic drag [12]. These resistive forces reduce vehicle efficiency and speed while increasing fuel consumption. Many observation methods have been developed and applied to address this issue. Load torque identification methods include model reference adaptive control (MRAC) [13], Kalman filters [14], and sliding mode observer (SMO) [15]. Due to its simplicity and robustness in the face of uncertainties and disturbances, SMO is increasingly receiving attention. Sliding mode observers comprise methods such as the disturbance observer, delayed output observer, extended state observer (ESO), integral-chain differentiator, and high-gain observer (HGO) [16]. Among these observers, ESO is tasked with monitoring and estimating direct disturbances and errors in modelling the object compared to reality. Thus, even with a model with low accuracy, it is still possible to design a good-quality controller, thereby indirectly simplifying the model. Any differences in the model will not affect the control mechanisms, including all disturbances in the extended state variables [17].

Hongxia and Jingtao [18] propose a method for estimating motor load torque and speed using an adaptive extended Kalman filter (AEKF), where the covariance matrix of noise is estimated. In contrast, the speed and load torque of the induction motor are estimated by EKF [18]. Tami *et al.* [9] proposes a method for estimating rotor speed, load torque, and parameters of permanent magnet synchronous motors using extended state observer (ESO). Lian *et al.* [19] utilize a sliding mode observation-based load torque observation method and two methods for determining the inertia moment for PMSM drive systems. Miao *et al.* [20] in their work, apply torque estimation and maximum torque per ampere (MTPA) fitting strategies using a freshly developed model for IPM synchronous machines. Manh *et al.* [21] apply HGO-based sensor less control for speed control of bearing-less synchronous motors. Kim *et al.* [22] uses a minimized disturbance observer proposed to mitigate the effects of DC offset and harmonic distortion by deploying adaptive frequency observation observers. Wang *et al.* [23] presents an adaptive sliding mode control (SMC) method combined with a disturbance torque observer (DTO).

However, the above works have not proposed a backstepping controller for the motor speed loop nor applied the ESO method to observe the load torque. Therefore, this paper proposes the design of a backstepping controller for a speed loop combined with a load torque observer, specifically an ESO, for IPM synchronous motors used in electric vehicles. Finally, the accuracy of the proposed methods will be verified through simulation results obtained using MATLAB/Simulink software.

2. MODELING THE ELECTRIC VEHICLE SYSTEM

2.1. The mathematical model of the IPM motor

In the d - q coordinate system, the IPMSM model can be represented as (1) [24], [25]:

$$\begin{cases} \frac{di_{sd}}{dt} = -\frac{1}{T_{sd}}i_{sd} + \omega_s \frac{L_{sq}}{L_{sd}}i_{sq} + \frac{1}{L_{sd}}U_{sd} \\ \frac{di_{sq}}{dt} = -\omega_s \frac{L_{sq}}{L_{sd}}i_{sd} - \frac{1}{T_{sq}}i_{sq} + \frac{1}{L_{sq}}U_{sq} - \omega_s \frac{\psi_p}{L_{sq}} \\ \psi_{sd} = L_{sd}i_{sd} + \psi_p \\ \psi_{sq} = L_{sq}i_{sq} \\ T_e = \frac{3}{2}p_p(\psi_p i_{sq} - i_{sd}i_{sq}(L_{sd} - L_{sq})) \\ T_e - T_L = \frac{J}{p_p} \frac{d\omega}{dt} \end{cases} \quad (1)$$

where: U_{sd} and U_{sq} voltage in the d and q -axis stator frame, i_{sd} and i_{sq} is current in the d and q -axis stator frame, R_s is stator resistance, L_{sd} and L_{sq} is stator inductance in the d and q -axis, ω_s is the motor angular velocity, ψ_p is magneto motive force, p_p is several motor poles, T_e is output torque of the motor; ψ_{sd}, ψ_{sq} are Stator flux linkage on the d and q -axis; T_L is load torque, J is rotor inertia, $T_{sd} = \frac{L_{sd}}{R_s}$ is stator d -axis time constant, $T_{sq} = \frac{L_{sq}}{R_s}$ stator q -axis time constant.

2.2. Modeling the forces acting on the car

When a car is running on the road, there are several primary types of resistance forces, which is shown in Figure 1: rolling resistance, frictional resistance, air resistance, and inertia. Frictional resistance is typically much smaller than the other components, so it will be neglected in the model [12]. The air resistance is calculated according to the formula:

$$F_{wind} = \frac{1}{2} \rho C_d A_f (v_{veh} + v_{wind})^2 \quad (2)$$

The rolling friction force can be calculated as follows (considering rolling friction on a rigid surface):

$$F_{roll} = f_r m_v g \cos \alpha \quad (1)$$

with:

$$f_r = 0.01 \left(1 + \frac{3.6}{100} v_{veh} \right) \quad (2)$$

where: ρ is the air density; C_d is the coefficient of air resistance (typically: $0.2 < C_d < 0.4$); A_f is the frontal area of the vehicle's body (cross-sectional area); v_{wind} is the wind speed; g is gravitational acceleration; α is gradient; f_r rolling resistance coefficient; v_{veh} is the vehicle speed.

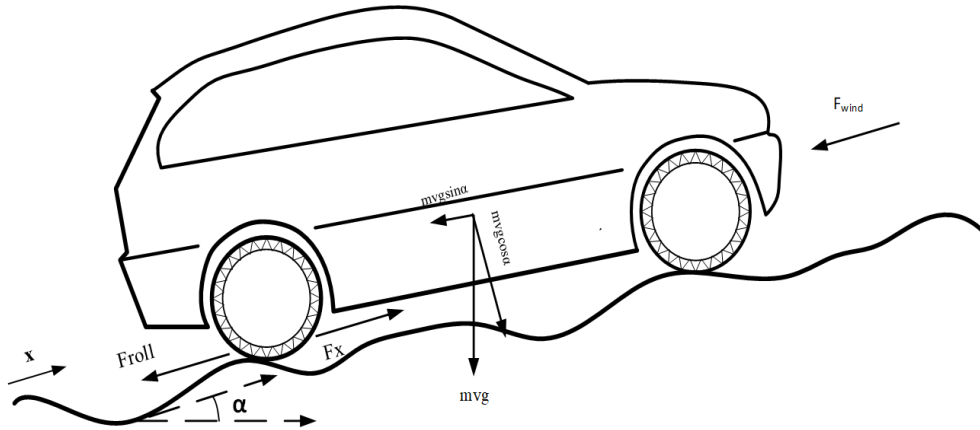


Figure 1. The forces acting on an electric car

3. CONTROL DESIGN

Figure 2 depicts the control structure based on field-oriented control (FOC) for the IPM motor applied in electric vehicles. The structure utilises a PI controller for current control and the backstepping method for the speed controller for the speed loop to enhance system stability. Additionally, the extended observer is used to monitor the load torque, facilitating the accurate estimation of disturbances and environmental effects.

3.1. Designing the load torque observer - extended state observer

When controlling IPM motors, understanding every state is the key to smooth and efficient operation. To achieve this, we need an observer-the ESO. This observer helps us monitor what cannot be directly observed, aiding in smoother and more robust motor operation. ESO method is designed as follows [16].

$$\begin{cases} \dot{\hat{x}}_1 = \hat{x}_2 + \frac{\alpha_1}{\varepsilon} (y - \hat{x}_1) \\ \dot{\hat{x}}_2 = bu + \hat{\sigma} + \frac{\alpha_2}{\varepsilon^2} (y - \hat{x}_1) \\ \dot{\hat{\sigma}} = \frac{\alpha_3}{\varepsilon^3} (y - \hat{x}_1) \end{cases} \quad (5)$$

Where $\hat{x}_1, \hat{x}_2, \hat{\sigma}$ are the observer states, $\varepsilon > 0$ is the gain, $(y - \hat{x}_1)$ is the observation error, u is the control input, $\alpha_1, \alpha_2, \alpha_3$ are positive constants satisfying the Hurwitz stability criterion. From the motion in [1]:

$$T_e - T_L = \frac{J}{p} \frac{d\omega}{dt} \Rightarrow \frac{d\omega}{dt} = \frac{p}{J} (T_e - T_L) \Rightarrow \dot{\omega} = \frac{p}{J} T_e - \frac{p}{J} T_L \quad (6)$$

Substituting [5], we obtain:

$$\begin{cases} \dot{\hat{\omega}} = \frac{p}{J} T_e + \hat{\sigma} + \frac{\alpha_2}{\varepsilon^2} (\omega - \hat{\omega}) \\ \dot{\hat{\sigma}} = \frac{\alpha_3}{\varepsilon^3} (\omega - \hat{\omega}) = -\frac{p}{J} T_L \Rightarrow T_L = -\frac{J\alpha_3}{p\varepsilon^3} (\omega - \hat{\omega}) \end{cases} \quad (7)$$

The stability can be proved as follows: The error between the actual values and the observed values is found by the vector as (8):

$$\eta = [\eta_1 \ \eta_2 \ \eta_3]^T \quad (8)$$

where:

$$\eta_1 = \frac{x_1 - \hat{x}_1}{\varepsilon^2}; \eta_2 = \frac{x_2 - \hat{x}_2}{\varepsilon}; \eta_3 = f - \hat{\sigma} \quad (9)$$

Differentiating the error values, we obtain an equation in the form:

$$\varepsilon \dot{\eta} = \bar{A}\eta + \varepsilon \bar{B}\dot{f} \quad (3)$$

with:

$$A = \begin{pmatrix} -k_1 & 1 & 0 \\ -k_2 & 0 & 1 \\ -k_3 & 0 & 0 \end{pmatrix}$$

Considering the characteristic equation of matrix A, we have:

$$|\lambda I - A| = \begin{vmatrix} \lambda + k_1 & -1 & 0 \\ k_2 & \lambda & -1 \\ k_3 & 0 & \lambda \end{vmatrix} = 0 \quad (11)$$

From in [11], we obtain:

$$\lambda^3 + k_1\lambda^2 + k_2\lambda + k_3 = 0 \quad (12)$$

Choose k_1, k_2, k_3 such that A is Hurwitz; there exists a unique positive definite, symmetric matrix P satisfying the Lyapunov function for every positive definite, symmetric matrix Q given as (13).

$$A^T + PA + Q = 0 \quad (13)$$

Choose the Lyapunov function as (14).

$$V_0 = \varepsilon \eta^T P \eta \quad (14)$$

Taking the derivative of V_0 , we obtain:

$$\begin{aligned} \dot{V}_0 &= \varepsilon \dot{\eta}^T P \eta + \varepsilon \eta^T P \dot{\eta} = (\bar{A}\eta + \varepsilon \bar{B}\dot{f})^T P \eta + \eta^T P (\bar{A}\eta + \varepsilon \bar{B}\dot{f}) \\ &= \eta^T \bar{A}^T P \eta + \varepsilon (\bar{B}\dot{f})^T P \eta + \eta^T \bar{A} P \eta + \varepsilon \eta^T P \bar{B} \dot{f} \\ &= \eta^T (\bar{A}^T P + P \bar{A}) \eta + 2\varepsilon \eta^T P \bar{B} \dot{f} \leq \eta^T Q \eta + 2\varepsilon \|P \bar{B}\| \|\eta\| \|\dot{f}\| \end{aligned} \quad (15)$$

and

$$\dot{V}_0 \leq -\lambda \|\eta\|^2 \|P \bar{B}\| \|\eta\|_{\min} \quad (16)$$

where $-\lambda_{\min}$ is the smallest eigenvalue of Q. To ensure $\dot{V}_0 \leq 0$, the coefficient ε is chosen to satisfy the conditions:

$$\lambda \|\eta\|^2 \|P\bar{B}\| \|\eta\|_{min} \tag{17}$$

In this case, the observation error η will converge to the vicinity of ε . Therefore, the stability of the method has been proven.

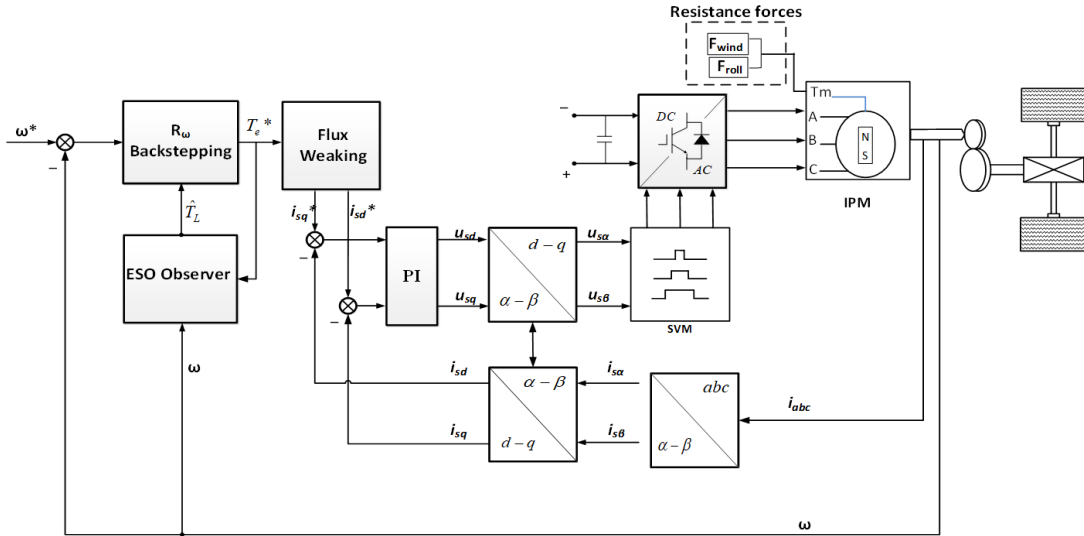


Figure 2. The FOC control structure for the IPM motor in an electric car

3.2. Designing a backstepping controller for the speed loop

Backstepping is a straightforward method that can be effectively applied to nonlinear systems. It employs Lyapunov's method to select control signals, driving the controlled variable towards the desired value. Starting from in (1) and applying the Backstepping theory, with the error signal defined as e , we have:

$$e = \omega^* - \omega \tag{18}$$

Taking the derivative of both sides, we obtain:

$$\dot{e} = \dot{\omega}^* - \dot{\omega} = \dot{\omega}^* - \frac{p_p}{J} (T_e - T_L) \tag{19}$$

According to the Lyapunov stability criterion, a positive definite function V_1 is required to stabilize in (19) at the origin. Thus, the function V_1 is chosen as (20).

$$V_1 = \frac{1}{2} e^2 \tag{20}$$

Taking the derivative of V_1 , we obtain $\dot{V}_1 = e \cdot \dot{e}$. Choose the control parameter $k > 0$ such that:

$$\dot{e} = -ke \Rightarrow \dot{V}_1 = e \cdot (-ke) = -ke^2 < 0 \tag{21}$$

Substituting into in (20), we obtain:

$$\dot{\omega}^* - \frac{p_p}{J} (T_e - T_L) = -ke \Rightarrow T_e = T_L + \frac{J}{p_p} (ke + \dot{\omega}^*) \tag{22}$$

Where J is the inertia, p_p is the pole pair, and T_L is the load torque estimated by the ESO designed in section 3.1.

4. SIMULATION RESULTS

Part 4 presents simulation results of responses, including speed, currents, electromagnetic torque, estimated load torque, and actual load torque, to verify the advantages of the backstepping controller for

speed control combined with the ESO for the electric car, as shown in Figure 1. Simulation parameters were collected from the IPM traction motor, and the car's specifications are in Tables 1 and 2.

The speed response in Figure 3 uses the backstepping control method, and the feedback speed closely follows the reference speed. Backstepping has effectively adjusted the motor speed to match the reference speed. However, at the initial startup, the feedback speed oscillates around 0.15 s, as the transition from acceleration to steady-state and even deceleration has a slight overshoot, but this is very small, insignificant, and quickly returns to track the set value. This demonstrates the controller's ability to handle sudden changes such as acceleration and deceleration. Overall, with the motor's speed response, as shown above, we can see that the system, using the BSP controller, exhibits good stability even in the presence of disturbances and external factors.

Figure 4 illustrates the results of the currents i_{sd} and i_{sq} . From these results, we can observe that the two currents, i_{sd} and i_{sq} , have been successfully decoupled. The i_{sd} current has been controlled to be less than 0, allowing the motor to generate a large torque even when operating at speeds higher than the rated speed.

Table 1. Parameters of the IPM motor

Parameters	Symbols	Values
Stator resistance	R_s	$6.5e-3$ (Ohm)
d -axis inductance	L_{sd}	$1.597e-3$ (H)
q -axis inductance	L_{sq}	$2.057e-3$ (H)
Inertia	J	0.09 (kg.m ²)
Pole pairs	p_p	4
DC voltage	V_{dc}	550 (V)

Table 2. The specifications of an electric car

Parameters	Values	Units
Vehicle + load mass	2018	Kg
Wheel radius	0.3	m
Transmission ratio	9.73	
Maximum speed	130	Km/h
Density of air	1.25	Km/m ³
Rolling resistance coefficient	0.02	

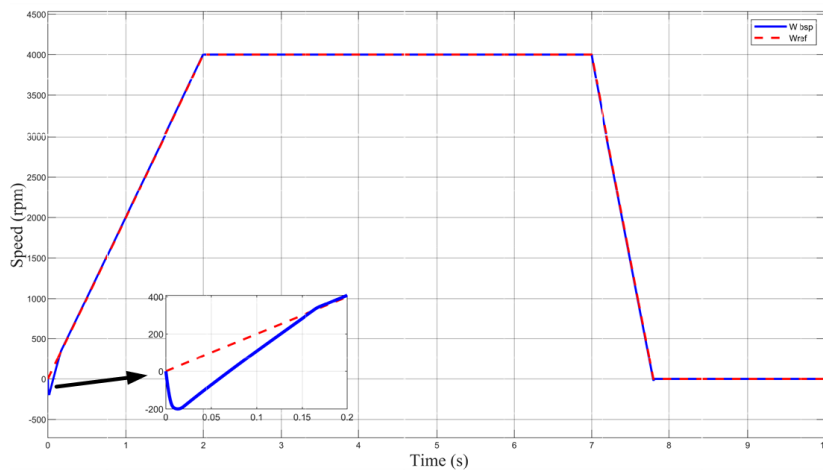


Figure 3. Speed response using the backstepping controller

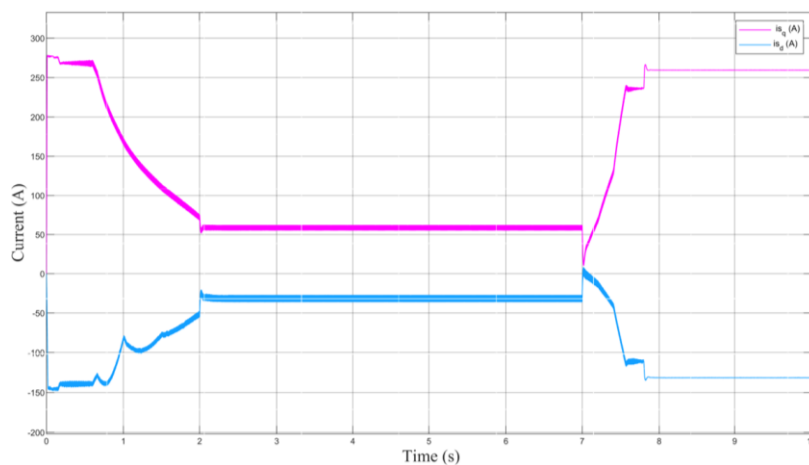


Figure 4. The results of the currents I_{sd} - I_{sq}

In Figure 5, at $t = 0.2$ s, corresponding to the rated speed of 1200 rpm, the torque tends to decrease to allow for acceleration, as the voltage has reached the rated level and cannot increase further. This is particularly suitable for electric vehicles, as optimizing the torque curve helps enhance the motor's efficiency and performance while minimizing energy consumption.

Figure 6 shows that the observed torque results closely match the actual values. At state transition points, the observed values oscillate slightly but quickly return to closely follow the actual values. This positive outcome indicates that the observer has accurately and effectively estimated the torque curve. The similarity between the observed and actual torque curves indicates that the observation system responds well to environmental changes and can accurately estimate torque under various conditions.

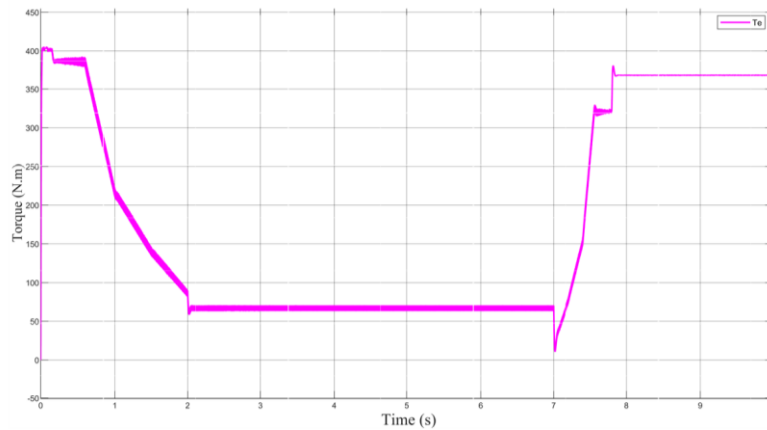


Figure 5. The results of the electromagnetic torque

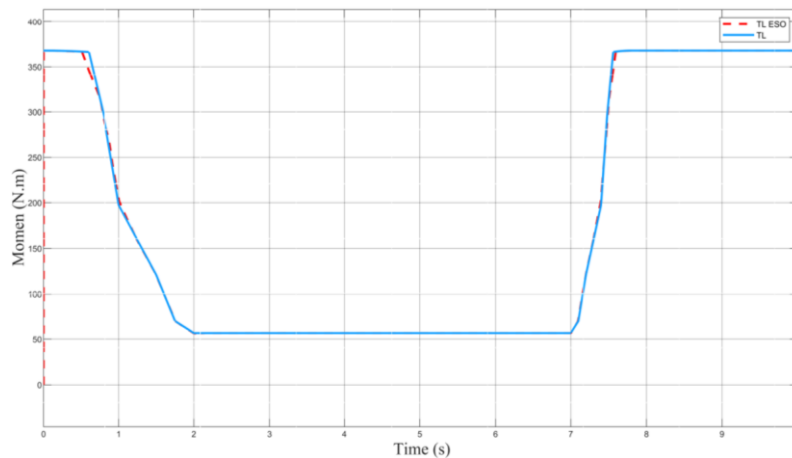


Figure 6. Torque estimated using ESO and actual torque

5. CONCLUSION

This study introduces the backstepping control method for the speed control loop and the extended state observer (ESO) to enhance stability in IPM motors for electric vehicles. Using the Backstepping method, a robust controller has been designed to minimise errors in controlling the speed of the IPM motor, significantly improving the accuracy and response of the system. Additionally, the integration of the extended state observer (ESO) enables the estimation of load torque, allowing for the consideration of uncertainties such as changes in operating conditions, external disturbances, and other factors that may affect the motor's stability in actual operating situations. Simulation results have demonstrated the validity of the proposed control methods in controlling the IPM motor's speed while mitigating the effects of load torque. Ultimately, this research contributes to the development of more advanced control methods and automatic control systems for electric vehicles and related industrial applications.

FUNDING INFORMATION

Our paper is financially supported by the University of Transport and Communications (UTC) and Thuyloi University.

AUTHOR CONTRIBUTIONS STATEMENT

This journal uses the Contributor Roles Taxonomy (CRediT) to recognize individual author contributions, reduce authorship disputes, and facilitate collaboration.

Name of Author	C	M	So	Va	Fo	I	R	D	O	E	Vi	Su	P	Fu
An Thi Hoai Thu Anh	✓	✓	✓	✓	✓	✓		✓	✓	✓				✓
Tran Hung Cuong		✓	✓			✓	✓	✓	✓	✓	✓	✓		
Nguyen Van Hoa			✓		✓	✓			✓	✓				

C : **C**onceptualization

M : **M**ethodology

So : **S**oftware

Va : **V**alidation

Fo : **F**ormal analysis

I : **I**nterpretation

R : **R**esources

D : **D**ata Curation

O : **O**riginal Draft

E : **E**xperimentation

Vi : **V**isualization

Su : **S**upervision

P : **P**roject administration

Fu : **F**unding acquisition

CONFLICT OF INTEREST STATEMENT

Authors state no conflict of interest.

DATA AVAILABILITY

The data that support the findings of this study are openly available in this paper.




REFERENCES

- [1] T. Wan, Z. Chen, and D. Liu, "Research on user characteristics and demand trend evolution of compact hybrid electric cars," *Journal of Innovation and Development*, vol. 1, no. 1, pp. 24–28, 2022, doi: 10.54097/jid.v1i1.3794.
- [2] Y. Liu, B. Zhou, and S. Fang, "Sliding mode control of PMSM based on a novel disturbance observer," in *2009 4th IEEE Conference on Industrial Electronics and Applications, ICIEA 2009*, 2009, pp. 1990–1994. doi: 10.1109/ICIEA.2009.5138551.
- [3] L. Sun, X. Zhang, L. Sun, and K. Zhao, "Nonlinear speed control for PMSM system using sliding-mode control and disturbance compensation techniques," *IEEE Transactions on Power Electronics*, vol. 28, no. 3, pp. 1358–1365, 2013, doi: 10.1109/TPEL.2012.2206610.
- [4] N. J. Patil, D. R. H. Chile, and D. L. M. Waghmare, "Fuzzy adaptive controllers for speed control of PMSM drive," *International Journal of Computer Applications*, vol. 1, no. 11, pp. 91–98, 2010, doi: 10.5120/233-387.
- [5] M. Singh and A. Chandra, "Application of adaptive network-based fuzzy inference system for sensor less control of PMG-based wind turbine with nonlinear-load-compensation capabilities," *IEEE Transactions on Power Electronics*, vol. 26, no. 1, pp. 165–175, 2011, doi: 10.1109/TPEL.2010.2054113.
- [6] R. J. Wai and H. H. Chang, "Backstepping wavelet neural network control for indirect field-oriented induction motor drive," *IEEE Transactions on Neural Networks*, vol. 15, no. 2, pp. 367–382, 2004, doi: 10.1109/TNN.2004.824411.
- [7] N. M. Neya, S. Saberi, and B. Mozafari, "Direct predictive speed control of permanent magnet synchronous motor fed by matrix converter," *International Journal of Power Electronics and Drive Systems*, vol. 11, no. 4, pp. 2183–2193, 2020, doi: 10.11591/ijpeds.v11.i4.pp2183-2193.
- [8] M. Karabacak and H. I. Eskikurt, "Speed and current regulation of a permanent magnet synchronous motor via nonlinear and adaptive backstepping control," *Mathematical and Computer Modelling*, vol. 53, no. 9–10, pp. 2015–2030, 2011, doi: 10.1016/j.mcm.2011.01.039.
- [9] R. Tami, D. Boutat, G. Zheng, F. Kratz, and R. El Gouri, "Rotor speed, load torque and parameters estimations of a permanent magnet synchronous motor using extended observer forms," *IET Control Theory and Applications*, vol. 11, no. 9, pp. 1485–1492, 2017, doi: 10.1049/iet-cta.2016.0226.
- [10] K. Horvath and M. Kuslits, "Model-based development of induction motor control algorithms with modular architecture," in *Proceedings - 2016 IEEE International Power Electronics and Motion Control Conference, PEMC 2016*, 2016, pp. 133–138. doi: 10.1109/EPEPEMC.2016.7751987.
- [11] G. Kujundžić, M. Vašak, and J. Matuško, "Estimation of vrla battery states and parameters using sigma-point Kalman filter," in *IEEC*, 2015, pp. 204–211. doi: 10.1109/EDPE.2015.7325295.
- [12] S. Krishnamoorthy and P. P. K. Panikkar, "A comprehensive review of different electric motors for electric vehicles application," *International Journal of Power Electronics and Drive Systems (IJPEDS)*, vol. 15, no. 1, pp. 74–90, 2024, doi: 10.11591/ijpeds.v15.i1.pp74-90.
- [13] Suryakant, M. Sreejeth, and M. Singh, "Improved anfis-based MRAC observer for sensor less control of PMSM," *Journal of Intelligent and Fuzzy Systems*, vol. 42, no. 2, pp. 1061–1073, 2022, doi: 10.3233/JIFS-189772.
- [14] P. Niedermayr, L. Alberti, S. Bolognani, and R. Abl, "Implementation and experimental validation of ultrahigh-speed PMSM sensor less control by means of extended Kalman filter," *IEEE Journal of Emerging and Selected Topics in Power Electronics*, vol. 10, no. 3, pp. 3337–3344, Nov. 2022, doi: 10.1109/JESTPE.2020.3041026.




- [15] H. Ding, X. Zou, and J. Li, "Sensor less control strategy of permanent magnet synchronous motor based on fuzzy sliding mode observer," *IEEE Access*, vol. 10, pp. 36743–36752, 2022, doi: 10.1109/ACCESS.2022.3164519.
- [16] J. Liu and X. Wang, *Adaptive sliding mode control for mechanical systems*. China, 2011. doi: 10.1007/978-3-642-20907-9_6.
- [17] T. P. Van and K. T. Van, "Discussion on the active disturbance rejection control (ADRC) method," in *ISSN*, 2015, pp. 61–65.
- [18] Y. Hongxia and H. Jingtao, "Speed and load torque estimation of induction motors based on an adaptive extended Kalman filter," *IEEC*, vol. 433, no. 440, pp. 433–440, Jan. 2012.
- [19] C. Lian, F. Xiao, S. Gao, and J. Liu, "Load torque and moment of inertia identification for permanent magnet synchronous motor drives based on sliding mode observer," *IEEE Transactions on Power Electronics*, vol. 34, no. 6, pp. 5675–5683, Jun. 2019, doi: 10.1109/TPEL.2018.2870078.
- [20] Y. Miao, H. Ge, M. Preindl, J. Ye, B. Cheng, and A. Emadi, "MTPA fitting and torque estimation technique based on a new flux-linkage model for interior-permanent-magnet synchronous machines," *IEEE Transactions on Industry Applications*, vol. 53, no. 6, pp. 5451–5460, Jun. 2017, doi: 10.1109/TIA.2017.2726980.
- [21] T. N. Manh, D. Q. Pham, D. N. Quang, and L. N. Tung, "Sensorless speed control of PMSM–magnetic bearing using high-gain observer," *MC&A*, vol. 1, no. 1, Jun. 2020.
- [22] H. S. Kim, S. K. Sul, H. Yoo, and J. Oh, "Distortion-minimizing flux observer for IPMSM based on frequency-adaptive observers," *IEEE Transactions on Power Electronics*, vol. 35, no. 2, pp. 2077–2087, Jun. 2020, doi: 10.1109/TPEL.2019.2920691.
- [23] Q. Wang, H. Yu, M. Wang, and X. Qi, "An improved sliding mode control using disturbance torque observer for permanent magnet synchronous motor," *IEEE Access*, vol. 7, pp. 36691–36701, Mar. 2019, doi: 10.1109/ACCESS.2019.2903439.
- [24] Z. Zhang and X. Liu, "A duty ratio control strategy to reduce both torque and flux ripples of DTC for permanent magnet synchronous machines," *IEEE Access*, vol. 7, pp. 11820–11828, Jan. 2019, doi: 10.1109/ACCESS.2019.2892121.
- [25] H. Wang, C. Li, G. Zhang, Q. Geng, and T. Shi, "Maximum torque per ampere (MTPA) control of IPMSM systems based on controller parameters self-modification," *IEEE Transactions on Vehicular Technology*, vol. 69, no. 3, pp. 2613–2620, Jan. 2020, doi: 10.1109/TVT.2020.2968133.

BIOGRAPHIES OF AUTHORS






An Thi Hoai Thu Anh    received her Engineer (1997) and M.Sc. (2002) degrees in Industrial Automation Engineering from Hanoi University of Science and Technology and completed Ph.D. degree in 2020 from The University of Transport and Communications (UTC). Now, she is a lecturer at the Faculty of Electrical and Electronic Engineering at the University of Transport and Communications (UTC). Her interests include controlling power electronic converters, controlling electric motor drives, and saving energy solutions for industry and transportation. She can be contacted at email: htanh.ktd@utc.edu.vn.



Tran Hung Cuong    received his Engineer (2010); and M.Sc. (2013) degrees in Industrial Automation Engineering from Hanoi University of Science and Technology and completed Ph.D. degree in 2020 from Hanoi University of Science (HUST). Now, he is a lecturer at the Faculty of Electrical and Electronic Engineering at Thuy Loi University (TLU). His current interests include power electronic converters and electric motor drives, converting electricity from renewable energy sources to the grid, and saving energy solutions for the grid and transportation. He can be contacted at email: cuongh@tlu.edu.vn.



Nguyen Van Hoa    is a fourth-year student majoring in Electrical Engineering at the University of Transport and Communications (UTC), Vietnam. His current interests include power electronics and electric drive control, which are applied in the transportation and industry. He can be contacted at email: hoa201503763@lms.utc.edu.vn.